Enhanced near infrared emission in water-soluble NdF_3 nanocrystals by Ba^{2+} doping

Ting Fan (樊 婷), Qinyuan Zhang (张勤远)*, and Zhonghong Jiang (姜中宏)

MOE Key Laboratory of Special Functional Materials and Institute of Optical Communication Materials, South China University of Technology, Guangzhou 510641, China

**Corresponding author: qyzhang@scut.edu.cn*

Received May 20, 2011; accepted July 12, 2011; posted online September 22, 2011

A simple and efficient method for the synthesis of water-soluble NdF_3 and NdF_3:Ba^{2+} nanocrystals under hydrothermal conditions is established. The method involves the coating of the nanocrystals with a layer of hydrophilic polymer polyvinylpyrrolidone (PVP). The as-prepared products are characterized by powder X-ray diffraction, field emission scanning electronic microscopy, Fourier transform infrared spectroscopy, and photoluminescence spectroscopy. The PVP coating transforms the nanocrystals into a biocompatible material and improves the fluorescence intensity of NdF_3 in the near infrared (NIR) region. The morphology of the nanoparticles changes, whereas the fluorescence intensity of NdF_3 in the NIR region increases when a small amount of Ba^{2+} is doped into the NdF_3/PVP nanoparticles.

OCIS codes: 160.0160, 160.2540, 160.4236, 160.4670.

doi: 10.3788/COL201210.021602.

The application of fluorescent labeling materials has significantly stimulated the study of complex biological interactions in the field of biology[1]. Traditional bio-labels such as organic dyes and quantum dots (QDs) have inevitable limitations. Most organic dyes exhibit weak photostability and broad emission bands, whereas QDs are affected by potential toxicity, chemical instability, and short luminescence lifetimes[2]. Recently, trivalent lanthanide (Ln^{3+}) doped nanoparticles have been proposed as a new class of material for biological fluorescent labeling because of their attractive optical and chemical features[3−6]. For in vivo imaging, the use of bio-labels with both excitation and emission bands in the near infrared (NIR) region has been proposed because biological tissues are relatively transparent in the NIR spectral range and less damage under excitation in such range can affect the tissues[7−12].

Generally, to achieve highly efficient radiative emissions of the Ln^{3+} ions, competitive phonon-assisted nonradiative transitions should be inhibited fully. This requires a low phonon frequency host for the Ln^{3+} ions. NdF_3 nanoparticles have been proved to be independent of concentration quenching effect and possess very low phonon energy[13]. NdF_3 nanoparticles coated with silica shells have been used in in vivo detection. The high efficiency of fluorescence in the NIR region has been demonstrated[14]. The coating of silica can improve the fluorescence intensity of Nd^{3+}, which indicates its potential as an alternative material for bio-application. Currently, research on water-soluble NdF_3 nanoparticles is very limited. Coupled with the observation that fluorescence intensity is very weak when fluorescent labeling nanoparticles are dispersed in water, improving the photoluminescence of water-soluble nanoparticles is an urgent issue.

Codoping Ba^{2+} ions can improve the emission intensity of rare earth doped materials[15,16]. We present a one-step synthesis method where water-soluble NdF_3 and NdF_3:Ba^{2+} nanocrystals are coated with a layer of hydrophilic polymer polyvinylpyrrolidone (PVP) via a hydrothermal method. The coating of PVP makes the material biocompatible and improves the fluorescence intensity of NdF_3 in the NIR region. We doped divalent Ba^{2+} ions into the NdF_3/PVP nanoparticles and found that doping of Ba^{2+} can change the morphology of the nanoparticles and further improve the fluorescence intensity in the NIR region. The enhanced luminescence is valuable for application in *in vivo* NIR detection.

The reagents, including the PVP, $BaCl_2$, NH_4F, Nd_2O_3, and HNO_3, were of analytical grade and were used without further purification. The $Nd(NO_3)_3$ stock solutions (0.1 mol/L) were prepared by dissolving the Nd_2O_3 in concentrated HNO_3. In the typical procedure for the preparation of NdF_3 nanoparticles, 6 mL of 1-mol/L NH_4F solution was added to 20 mL of 0.1-mol/L $Nd(NO_3)_3$ solution. The mixture was transferred into a Telfon-lined stainless steel autoclave with 50 mL capacity. The sealed tank was heated in an oven to 160 °C and maintained for 10 h. Subsequently, the tank was taken out and cooled down to room temperature under ambient conditions. After the reactions, the composite samples were washed with deionized water and pure ethanol several times and then dried in an oven at 50 °C for 24 h. The NdF_3/polymer nanoparticles were prepared using the same procedure but with the addition of 0.3-g PVP into the solution at the initial stage. The NdF_3:Ba^{2+}/PVP nanoparticles were prepared by adding 0.3-g PVP and 5% $BaCl_2$ into the solution.

The powder X-ray diffraction (XRD) patterns were recorded by a diffractrometer (PW1830, philips) using Cu Kα irradiation at 40 kV and 40 mA. The morphologies were imaged by field emission scanning electron microscopy (FE-SEM) (NanoSEM 430, Nova) operating at 10 kV. The Fourier transform infrared (FT-IR) spectra were obtained using a FT-IR spectrometer (Vector 33, Bruker) over the 500–4 000-cm^{-1}

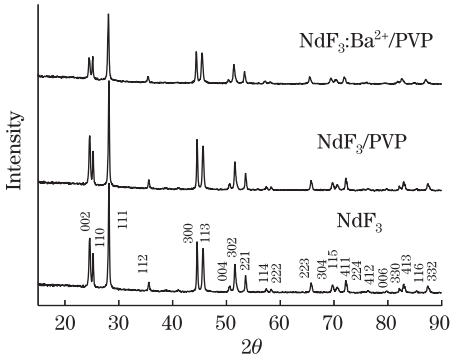

Fig. 1. XRD patterns of NdF_3, NdF_3/PVP, and NdF_3:Ba^{2+}/PVP nanoparticles.

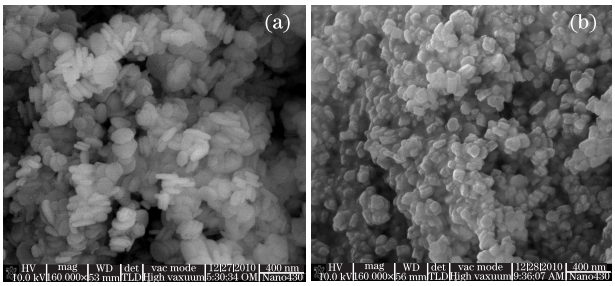

Fig. 2. FE-SEM images of (a) NdF_3/PVP and (b) NdF_3:Ba^{2+}/PVP nanoparticles.

region. The photoluminescence spectra were obtained at room temperature through a spectrometer (Triax320, Jobin-Yvon) with an 808-nm laser device (LD), as excitation source. The NIR luminescence of the samples was recorded with a liquid-nitrogen cooled InGaAs detector.

Figure 1 shows the typical XRD pattern of the synthesized nanoparticles. All the diffraction peaks can be readily indexed to the hexagonal NdF_3 phases with lattice constants $a = 0.7030$ and $c = 0.7199$ nm (JCPDS No. 9-416). No other impurity peaks were detected. The coating of PVP did not change the hexagonal phase of the nanoparticles and the doping Ba^{2+} ions completely entered the host lattice.

The FE-SEM images of NdF_3/PVP and NdF_3:Ba^{2+}-/PVP nanoparticles are shown in Fig. 2. The NdF_3/PVP particles are mono-dispersed nanoplates, as shown in Fig. 2 (a). The diameter and thickness of the plates are estimated to be 70 and 30 nm, respectively. When doped with Ba^{2+}, the diameter of the nanoparticles decreased to approximately 45 nm but the thickness did not change, as shown in Fig. 2 (b). This indicates that Ba^{2+} ions inhibited the growth of nanoparticles. The smaller size is beneficial in the use of biological labels.

The polymer layers on the surface of the nanoparticles were identified by FT-IR spectra, and the results are shown in Fig. 3. The band around 1 658 cm^{-1} can be assigned to the stretching vibrations of C=O of PVP, whereas the bands at 1 467–1 384 cm^{-1} can be assigned to the pyrollidone ring stretching vibrations of PVP. The appearance of the characteristic peaks indicates that the surface of NdF_3 nanoparticles was modified with a layer of polymer PVP. The presence of hydrophilic polymer coated on the surface caused the easy dispersion of functionalized nanoparticles in water and consequently, a homogenous colloidal solution was formed.

The fluorescence spectra of the samples under 808-nm laser excitation are shown in Fig. 4. The spectra represent three main transitions of the $^4F_{3/2} \rightarrow {}^4I_{9/2}$, $^4F_{3/2} \rightarrow {}^4I_{11/2}$, and $^4F_{3/2} \rightarrow {}^4I_{13/2}$ channels of Nd^{3+}. The coating of PVP layer increased the fluorescence intensity of NdF_3 at 1 049 nm by 16%. The increase could be attributed to the PVP layer, which prevented energy losses due to surface quenching[17].

When divalent Ba^{2+} ions were doped into the NdF_3/PVP nanoparticles, the fluorescence intensity increased further by 25% at 1 049 nm. It is well known that it is possible to tune the emission intensity by modifying the neighboring network design around rare earth ions by introducing other atoms into the host lattice. Incorporation of these metal atoms into the host lattice distorts the lattice to modifie the energy absorption and transfer behaviors, resulting in increased emission intensity[18−20]. A small amount of Ba^{2+} ions entered the lattice of Nd^{3+} completely and distorted the lattice network, resulting in an improvement in emission intensity.

In conclusion, we present a one-step synthesis method for water-soluble NdF_3 and NdF_3:Ba^{2+} nanocrystals, which involve coating with a layer of hydrophilic polymer PVP via hydrothermal method. The PVP coating causes the material to become biocompatible and improves the fluorescence intensity of NdF_3 in the NIR region. When a small amount of Ba^{2+} is doped into the NdF_3/ PVP nanoparticles, the diameter decreased, which could be beneficial for *in vivo* detection. The fluorescence intensity of NdF_3 in the NIR region increases because of the distorted lattice caused by Ba^{2+}. The

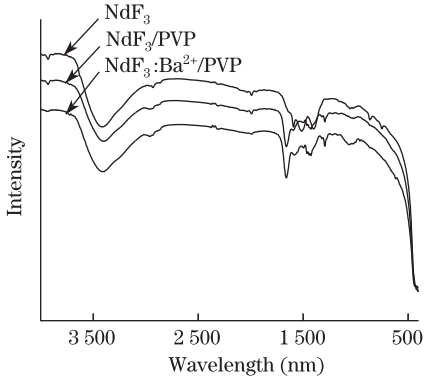

Fig. 3. FI-IR spectra of NdF_3, NdF_3/ PVP, and NdF_3:Ba^{2+}/PVP nanoparticles.

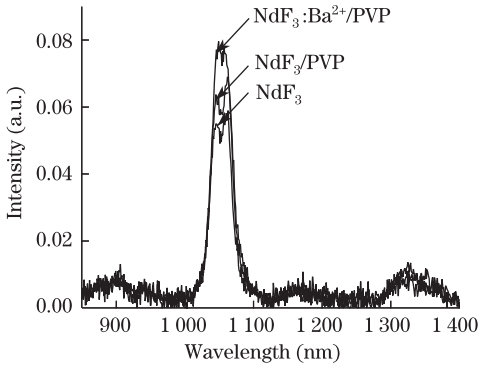

Fig. 4. Fluorescence spectra of NdF_3, NdF_3/PVP, and NdF_3:Ba^{2+}/PVP nanoparticles.

results are valuable for application in *in vivo* NIR detection.

This work was supported by the National Natural Science Foundation of China under Grant No. 50872036.

References

1. E. Schrock, S. duManoir, T. Veldman, B. Schoell, J. Wienberg, M. A. FergusonSmith, Y. Ning, D. H. Ledbetter, I. BarAm, D. Soenksen, Y. Garini, and T. Ried, Science **273,** 494 (1996).
2. T. Hyeon, J. Kim, and Y. Piao, Chem. Soc. Rev. **38,** 372 (2009).
3. X. G. Liu, F. Wang, and X. J. Xue, Angew. Chem. Int. Ed. **47,** 906 (2008).
4. J. C. G. Bunzli and C. Piguet, Chem. Soc. Rev. **34,** 1048 (2005).
5. X. G. Liu and F. Wang, J. Am. Chem. Soc. **130,** 5642 (2008).
6. X. Y. Chen, Q. A. Ju, W. Q. Luo, Y. S. Liu, H. M. Zhu, and R. F. Li, Nanoscale **2,** 1208 (2010).
7. X. G. Liu, F. Wang, D. Banerjee, Y. S. Liu, and X. Y. Chen, Analyst **135,** 1839 (2010).
8. W. B. Cai, D. W. Shin, K. Chen, O. Gheysens, Q. Z. Cao, S. X. Wang, S. S. Gambhir, and X. Y. Chen, Nano Lett. **6,** 669 (2006).
9. K. Konig, J. Microsc-oxford. **200,** 83 (2000).
10. F. Wang, W. Tan, Y. Zhang, X. Fan, and M. Wang, Nanotechnology **17,** R1 (2006).
11. Y. Zhang, X. Wang, D. Fei, N. Zhao, T. Zhao, H. Zhu, and L. Ding, Chin. Opt. Lett. **8,** 236 (2010).
12. M. Shi, H. Li, M. Pan, F. Su, L. Ma, P. Han, and H. Wang, Chin. Opt. Lett. **9,** 051901 (2011).
13. F. Bao, Y. S. Wang, Y. Cheng, and Y. H. Zheng, Mater. Lett. **60,** 389 (2006).
14. Q. Q. Wang, X. F. Yu, L. D. Chen, M. Li, M. Y. Xie, L. Zhou, and Y. Li, Adv. Mater. **20,** 4118 (2008).
15. L. H. Tian and S. Mho, J. Lumin. **122,** 99 (2007).
16. G. Wang, W. Qin, D. Zhang, L. Wang, G. Wei, P. Zhu, and R. Kim, J. Phys. Chem. C **112,** 17042 (2008).
17. G. Ghosh, M. K. Naskar, A. Patra, and M. Chatterjee, Opt. Mater. **28,** 1047 (2006).
18. T. Fan, Q. Zhang, and Z. Jiang, Opt. Commun. **284,** 1594 (2011).
19. R. Balakrishnaiah, D. W. Kim, S. S. Yi, K. Jang, H. S. Lee, and J. H. Jeong, Mater. Lett. **63,** 2063 (2009).
20. X. G. Liu, F. Wang, Y. Han, C. S. Lim, Y. H. Lu, J. Wang, J. Xu, H. Y. Chen, C. Zhang, and M. H. Hong, Nature **463,** 1061 (2010).

